Enviado: 20/07/2022 *Recibido: 04/08/2022* *Aceptado: 22/09/2022*

UNIVERSIDAD DISTRITAL FRANCISCO JOSE DE CALDAS

VISIÓN ELECTRÓNICA

https://doi.org/10.14483/issn.2248-4728

VISIÓN ELECTRÓNICA

Implementation of a manufacturing cell in assembly of Hanoi tower

Implementación de una Celda de Manufactura en el Ensamble de una Torre de Hanói

Henry Beltrán-Cicery[1], Diego Rojas-Sarmiento[2], Fabián Barrera-Prieto[3]

Abstract

Technology in the modern world, has become a necessity electronic and mechanical parts are unified to become mechanisms, which are the facilitating devices of human life and work. A common problem in the fabrication of a product is the high costs of personnel and the physical limitations, an example is the production of the tower of Hanoi. Thus, taking into account the knowledge acquired of the different courses at the level of robotics, mechanics, electronics and programming, the design and construction of a manufacturing cell and its operating interface was carried out, which has as its main function the distribution and manipulation of the elements necessary for the assembly of a tower of Hanoi, to know the process that a company requires for the elaboration of a product in an automated way. For the development of this project, four different processes were considered, a supply stage through pneumatic circuits, machine vision algorithms for quality control of the parts involved in the assembly, a selection process and place developed by a Phantom type robot with 4 degrees of freedom and, finally, the delivery of

[1] Mechatronic Engineer, University ECCI, Colombia. Current position: University ECCI, Colombia. E-mail: henrye.beltranc@ecci.edu.co ORCID: https://orcid.org/0000-0002-5239-7594

[2] MSc. In Mechatronic Engineer, UMNG, Colombia. Current position: University ECCI, Colombia. E-mail: drojass@ecci.edu.co ORCID: https://oícid.oíg/0000-0002-2962-6061

[3] MSc. In Mechatronics Systems, Universidade de Brasília. Current position: University ECCI, Colombia. E-mail: fbarrerap@ecci.edu.co.

Cite this article as: H. Beltrán-Cicery, D. Rojas-Sarmiento, F. Barrera-Prieto, “Implementation of a manufacturing cell in assembly of Hanoi tower”, Visión Electrónica, vol. 16, no. 2, 2022.

the finished product by means of a conveyor belt for later packaging.

Keywords: Process automation, quality control, pick and place, Robotic arm, Machine vision.

Resumen

La tecnología en el mundo moderno se ha convertido en una necesidad la cual por medio de partes electrónicas y mecánicas se unifican para convertirse en mecanismos los cuales son capaces de facilitar la vida del ser humano y optimizar el trabajo. Un problema común en la producción de un bien son los altos costos del personal y las limitaciones físicas que estos tienen, un ejemplo claro es la producción de la torre de Hanoi. Es así como teniendo en cuenta los conocimientos adquiridos en los diferentes cursos a nivel de robótica, mecánica, electrónica y de programación se realizó el diseño y construcción de una celda de manufactura y su interfaz de operación, la cual tiene como función principal la distribución y manipulación de los elementos necesarios para el ensamblaje de una torre de Hanoi, con el fin de dar a conocer el proceso que requiere una compañía para la elaboración de un producto de manera automatizada. Para el desarrollo del presente proyecto se tuvieron en cuenta cuatro diferentes procesos, una etapa de abastecimiento a través de circuitos neumáticos con su respectivo compresor, algoritmos de visión de máquina en conjunto con una cámara oscura, mitigando los efectos de las variaciones en la luz ambiente, para la selección y el control de calidad de las piezas involucradas en el ensamblaje, un proceso de pick and place desarrollado por un robot de 4 grados de libertad y, por último, la entrega del producto terminado mediante una banda transportadora para su posterior embalaje.

Palabras clave: Automatización de procesos, Control de calidad, Pick and place, Robótica, Visión de máquina.

1. Introduction

In a generalized way, the concepts related to robotics of manipulators take place thanks to the approach of some branches of engineering and technological development such as electronics, mechanics and mechatronics. Thus, the official definition of an industrial robot given by the IFR (International Federation of Robotics) in conjunction with the ISO (International Organization for Standarizaztion) is: "Reprogrammable multi-purpose manipulator, which is automatically controlled and has three or more axes of motion."[1].

Using this definition as a starting point, it is possible to make the link between an industrial robot and any numerical control machine, because its architecture is basically constituted by mechanical links driven by actuators that obey the operation of previously programmed movement, to support tasks in flexible automation processes, such as assembly tasks [2], movement of materials [3] and even quality control. [4]

In recent years and with the arrival of the so-called fourth industrial revolution [5], advances have been made in different fields to facilitate the implementation and operation of industrial robots. One of these is the kinematic analysis through genetic algorithms presented in [6], where they use the *Screws* direct model to find the value that the joint variables should have and thus locate the TCP of the Mitsubishi MELFA RV-2A robot, without the need to calculate an analytical model for the inverse kinematics. There have also been works that seek to improve the interaction experience, such as the development of haptic interfaces with 6 degrees of freedom to deliver a force feedback based system to the user [7]. Some of the most popular artificial intelligence algorithms, such as neural networks, have been used to solve the direct and inverse kinematic problem of different robotic architectures, such as 6R manipulators [8] and parallel manipulators [9].

In other cases, the inclusion of intuitive operation interfaces oriented to mobile robots is sought through gesture and speech processing as shown in [10], where 5 commands (FORWARD, BACKWARD, LEFT, RIGTH, STOP) are used to control the navigation of a differential architecture robot. In [11], an operation and monitoring system capable of alerting the operator about the condition of some environmental variables, such as increase in temperature and pollution, is presented, establishing a means of communication between the robot and the operator. Computer vision is not far behind, being one of the most attractive methodologies for the classification and recognition of objects that an industrial robot must manipulate. For example, the work shown in [12] proposes a *pick and place* system based on image processing to establish the location of an object in three dimensions and thus reconfigure the position of the TCP. In [13], apples were classified into 4 levels depending on their internal and external characteristics through colorimetric analysis and a spectrometer, in order to be transported by a robotic manipulator according to their appearance and state of ripeness.

Taking into account the above, this paper shows the different stages for the design and development of a 4 degrees of freedom serial manipulator at scale for sorting and assembly tasks by machine vision, through machine vision, with the ability to build a tower of Hanoi. The image recognition and processing algorithm is able to detect 4 different colors and 4 different sizes for the robot to group and locate them according to their characteristics.

2. Methods and materials

The following section presents the structural phases of the project, which gradually allowed the achievement of the proposed objectives. The first one, the design and construction of the robotic arm, the second one dedicated to the artificial vision process and finally a user interface that allows the control of the system.

2.1. Phantom X Robot

For the design of the robotic arm we took into account the architecture of the Phantom X Reactor, which has 4 servomotors. The axis of the base is perpendicular to the support surface and in turn with the following three joints, leaving as a function to the base the rotation of the robot in the Z axis and the following three actuators as translation and orientation in the plane created, this plane allows an orientation in the form of a circle formed in the same by the end effector. For its construction was first performed the direct kinematics with the parameters of Denavit Hartenberg modified (DHM) as illustrated in Table 1, where the parameters necessary for the interpretation of the morphology of the robot are presented, the variables that act directly on the dimension and movement capacity of the robot are: L_n , representing the dimensions of the links calculated in the physical study of the robot and q_n as the rotations of each joint.

Link	**Θ_i(rad)**	**α_i(rad)**	**a_i(mm)**	**d_i(mm)**	**Offset (rad)**
1	q1	0	0	L1	0
2	q2	π/2	0	0	π/2
3	q3	0	L2	0	0
4	q4	0	L3	0	0

Table 8. modified Denavit Hartenberg parameters for the robot used. Source: Own.

For the design of the links, three dual-axis servo motors with an active load capacity of 15 $kg * cm$ and an angular displacement of 270° and for the base a servo motor with a capacity of 20 $kg * cm$ with the same angular displacement were used. Thus, the calculation of the dimensions for the links was performed taking into account that their length must support the static torque of the actuators, the weight of each servomotor and the material from which it is made, in this case aluminum. The calculation of the center of mass and weight of the robot from joint 2 to the end effector was simulated as shown in Figure 1.

With these data and equations (1) and (2) the value of the static torque was found:

$$\vec{T} = \vec{r} x \vec{F} = \vec{r} x (m * a). \quad (1)$$

$$Ts = 18.19cm * 0.2Kgf = 3,638\ kgf * cm \quad (2)$$

According to the Guide to servo motor sizing document the expression used to calculate the inertia torque is shown in equation (3), where it is explained if the acceleration is low, the inertia torque is equal to four times the static torque., with values Ts = 3.638 $kg * cm$ an inertia torque Ti = 14.552 $kg * cm$ was obtained.

$$Ti = 4 * Ts \quad (3)$$

For the selected servomotors it is not possible to control the speed and acceleration, so the torque needed to overcome the inertia cannot be calculated directly. However, with equations (4)-(6) it is possible to estimate the maximum angular acceleration required. The values of $_{Timmax}$ and Izz were calculated through Solid Works.

$$Ti = 4 * 3{,}638\ kg * cm = 14{,}552\ kg * cm \quad (4)$$

$$a_{max} = \frac{Ti_{max}}{Izz} \quad (5)$$

$$a_{max} = \frac{1.4715\ Nm}{7.902872x10^{-3} Kg * m^2} = 3{,}24866 \frac{rad}{s^2} \quad (6)$$

For the first joint, a surface was designed to transmit the load and weight of the robot to an axial bearing, and thus the first actuator only supports the inertia of the robotic arm. For the maximum acceleration of the first joint, the equation (6) is used, which results in an acceleration of $3.24866\ \frac{rad}{s2}$.

Therefore, with the acceleration data obtained, we proceeded to design the base with supports for its anchorage, in order to balance the system in any of its movements. Figure 1 shows the design of the robotic arm, where the base is shown with the anchor points.

Figure 1. Fully extended robotic arm. Source: own elaboration.

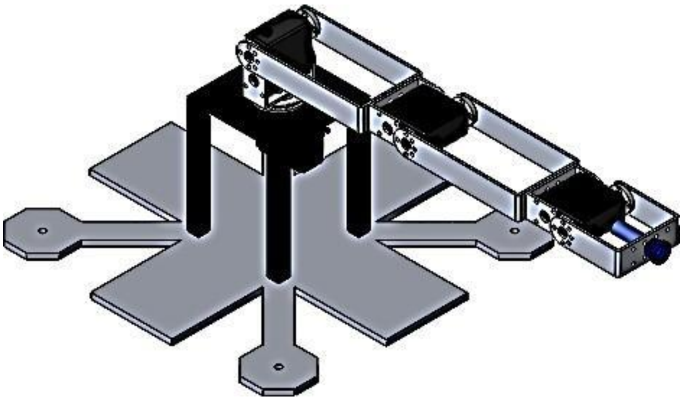

The next stage in the motion analysis for the 4R robot involves the calculation of the inverse kinematic problem. The first step is to determine from Figure 2 which actuators or joints are directly related to the final tool position, resulting in the first actuator giving the orientation of the end effector in the XY plane. The tool position vector is expressed as $Pt = [Pt_x , Pt_y . Pt]_z$

Once it was found that the first rotation affects this plane, it was concluded that the (θ_1) can be found by means of the equation 7

$$\theta_1 = atan2(\frac{Pt_y}{Pt_x}) \quad (7)$$

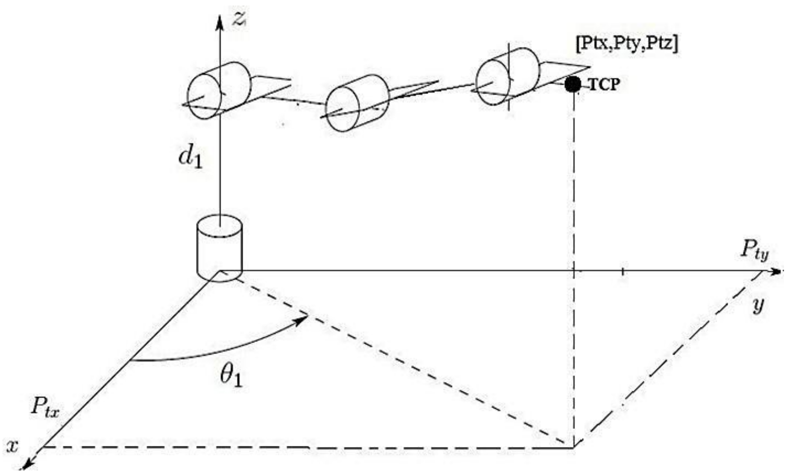

Figure 2. 3D geometric inverse of the Phantom. Source: own elaboration.

For the rest of the joints that are perpendicular to the robot surface and parallel to each other as previously explained, it was established that their rotation affects the orientation in the created plane, which was called ZR plane, as shown in Figure 3.

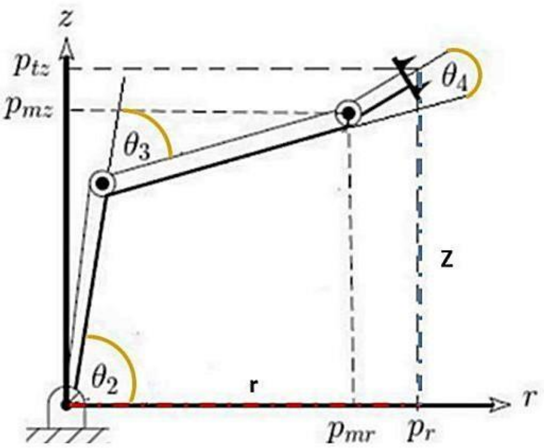

Figure 3. Geometric inverse of the Phantom in the ZR plane. Source: own elaboration.

From Figure 3 it was observed that the orientation of the tool in the ZR plane is directly affected by the movement of joints 2, 3 and 4, said statement mathematically is expressed as the sum of their angles (8).

$$\varphi = \theta_2 + \theta + \theta_3 + \theta_4 \qquad (8)$$

For the angles of rotations 2 and 3, by trigonometric functions, the Cartesian points of the end-effector (Pr) at the wrist (Pmr) were expressed by equations (9) and (10).

$$P_{mr} = P_r - d_4 \, Cos(\varphi) \qquad (9)$$

$$P_{mz} = Pt_z - d_4 \, sen(\varphi) - d_1 \qquad (10)$$

Where $P_r = \sqrt{(Pt\ )^2 + (Pt_y)^2}$, by reducing the system, it was analyzed that the links 2 and 3 form a triangle, for which the cosine theorem is used, found (11) the angle of rotation 3 (θ_3)

which is named as D.

$$Cos(\theta_3) = \frac{(p_{mz})^2 + (P_{mr})^2 - (d_2)^2 - (d_3)^2}{2 * d_2 * d_3} = D \quad (11)$$

To take into account the two possible solutions of the robot, elbow up and elbow down, the arc tangent function is used as shown in (14).

$$sen(\theta_3) = \pm\sqrt{1 - \cos(\theta_3)^2} \quad (12)$$

$$\tan(\theta_3) = \frac{sen(\theta_3)}{\cos(\theta_3)} \quad (13)$$

$$\theta_3 = \text{atan2}\left(\frac{\pm\sqrt{1 - D^2}}{D}\right) \quad (14)$$

Now for joint 2 (θ_2) an angle sum deduction was performed as a function of α and β as shown in Figure 4, where it can be seen that between joint four and the joint there is a triangular relationship, either elbow up or elbow down, with this relationship the cosine law can be applied to find the intermediate angle. It should be clarified that the *offset* must also be taken into account in this equation. Resulting in equations (15) and (16).

$$\alpha = atan2\left(\frac{P_{mz}}{P_{mr}}\right) \quad (15)$$

$$\beta = atan2\left(\frac{d_2 sen(\theta_3)}{d_2 + d_3\cos(\theta_3)}\right) \quad (16)$$

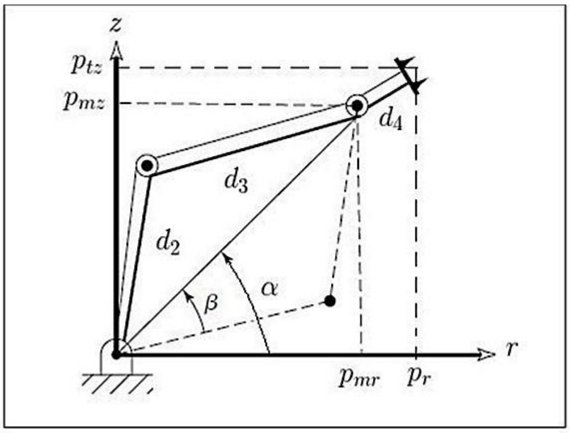

Figure 4. Derivation of the angle of rotation 2. Source: own.

With the results of α and β we cleared (17) the angle 2 (θ_2) and in turn we could find (18) the angle 4 (θ_4)

$$\theta_2 = \frac{\pi}{2} - \alpha - \beta \tag{17}$$

$$\theta_4 = \varphi - \theta_2 - \theta_3 \tag{18}$$

.

2.2. Machine vision

The Hanoi tower is composed of 5 pieces of different colors and sizes. For this task, morphological properties such as area and circularity of the piece were calculated, as well as color masks in HSV space for image binarization.

For image processing, the Matlab application called color *thresholder* was used, which provides the code that binarizes and identifies the selected color, separating it from the others. For this, an image is taken by means of a camera located in a dark capsule, in order to avoid variations in the light, as shown in figure 5, which by means of the lasso tool the green color is selected, resulting in the separation and identification of the color as shown in figure 6, where it can be observed that the object is discriminated from the other colors; although as it is observed there is noise due to reflection issues.

As can be seen, the system is not totally efficient, since it shows some noise which causes false positives in the process, which is why a filter was implemented for each area of the processed binary image, in addition to a dark chamber that aims to protect the image acquisition stage from the variation of ambient light. The filter discards the image, leaving only the color of the part as shown in Figure 7.

Figure 5. Image capture by means of the webcam. Source: own elaboration.

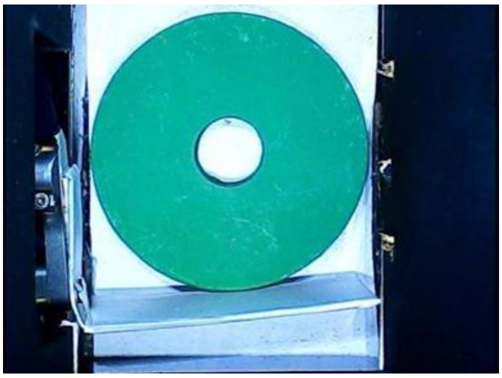

Figure 6. Color processing with noise. Source: own elaboration.

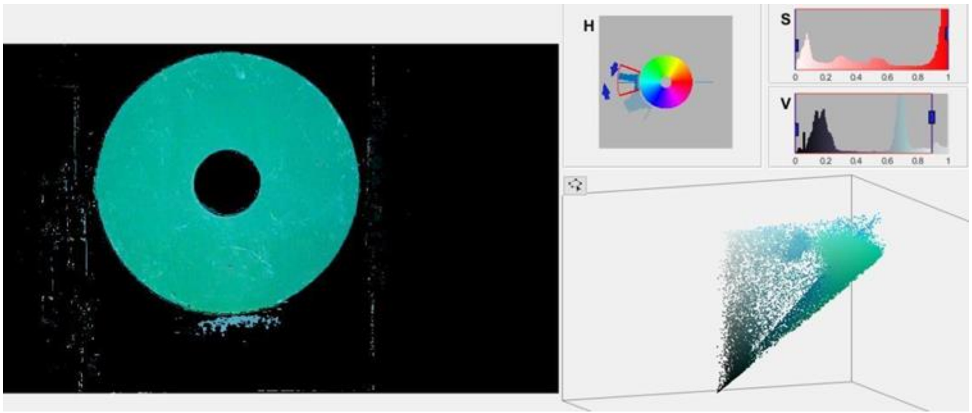

In the filtering by area, a threshold of 1000 pixels/in2 was used, resulting in the final segmentation shown in Figure 7.

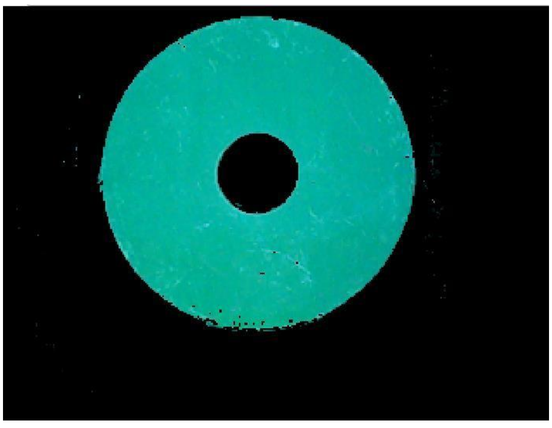

Figure 7. Image filtered by area. Source: own elaboration.

Once the color code is obtained, the same operation is performed for the remaining colors.

2.3. User interface

For the user interface, the parts mentioned above were unified as shown in **Figure 8**, where the complete system can be seen, consisting of the dark chamber, the pneumatic circuit, which consists of a double-acting cylinder with its respective 5/2 valve, and a suction cup to hold the parts, in addition to the robotic arm. Once the coupling was completed, the invention of the algorithm necessary to carry out the purpose of the project and the creation of the control panel which will have three buttons, where the *Start button* is responsible for starting the program at the required time, the second called *Clean Leds* is responsible for turning off the audio and visual signals of the system when it detects an unfit token according to established parameters, and finally, *Trajectory Test,* which is only allowed to be pressed the first 5 seconds after running the program, this in order to perform the trajectory of the robot making sure that the project is located in the established points, in addition, an interlock button was added which is responsible for performing the emergency stop operation.

Figure 9. Finished manufacturing cell. Source: own elaboration.

In addition, holes of approximately 1.3 mm in diameter are added on the entire surface of the manufacturing cell and a hole at the rear with a diameter of 1.5 cm, in order to create an air flow throughout the system and thus create an air cushion, which reduces the friction between the designed parts and the surface of the project.

Once the physical integration process is completed, a user interface is created (**Figure 10**), in which you can manually control the robot joints, the speed at which each end effect position change is executed, the connection to the Arduino, the transfer of any robot position to *home* and the robot trajectory for part gripping.

Figure 10. GUI with trajectory. Source: own elaboration.

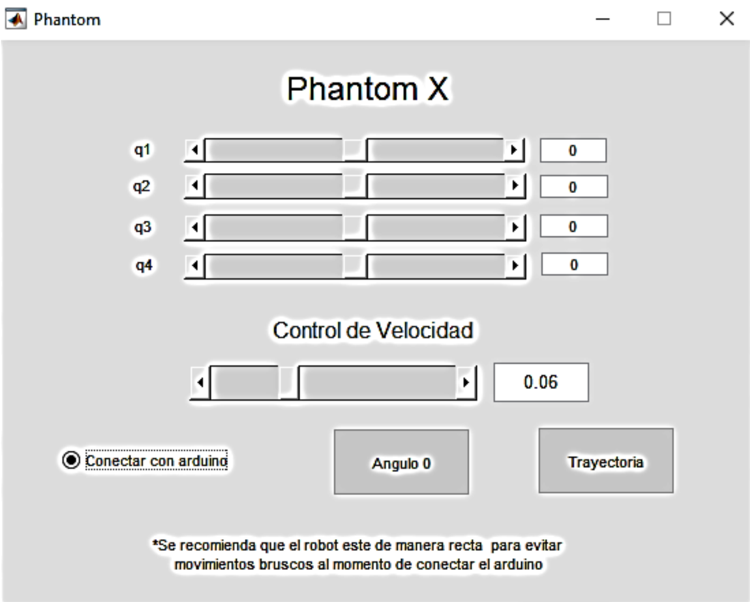

3. Results

The assembly of the Hanoi tower was achieved in which, by means of the different technological skills proposed, the whole process is carried out in approximately 4.5 minutes.

Friction was significantly reduced through the pneumatic process, which helps to protect part quality and distribution throughout the system.

Not being able to control the speed and acceleration of the robot, a stop was made at each point where the robot arrived, in order to perform an *on/off* control of the speed and acceleration, since, if the robot were to go from point to point without rest, this would increase its moment of inertia, stressing the servomotors more and eventually showing premature damage.

The graph in Figure 10 shows the path taken by each joint throughout the assembly process of the Hanoi tower, in which it can be seen that the joint with the longest path is number 1, because the actuator is the only one in charge of moving the robotic arm in a whole plane.

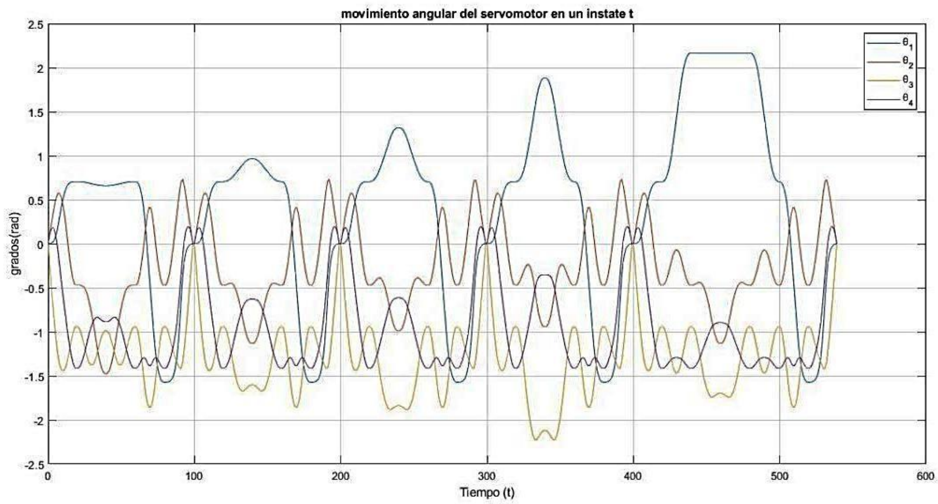

Figure 11. Graph of degree vs. time relationship for each of the parts. Source: own.

By means of the darkroom, the ambient light was reduced, which provided greater versatility in terms of reducing false positives when processing the image, since the light constant regularizes the color captured by the video camera.

The quality control of the parts was achieved by means of light and audio indicators, where it is possible to notify when a part is not suitable according to the previously stipulated parameters.

4. Conclusions

The CAD design provides a close idea of the physical prototype, since the simulation is carried out in an ideal way, without taking into account factors such as bubbles in the paint and wood bending due to humidity, among others. Therefore, it was necessary to make adjustments to the physical model during its construction.

By providing an air cushion to the manufacturing cell, the friction of the parts is reduced, maintaining the quality with which they come and at the same time allowing the parts to move throughout the process.

At the time of image processing, almost total control of the scene illumination was required, because variations in the ambient light increased the segmentation and identification error in the purple and blue pieces.

The robotic arm allows performing the necessary trajectories for the assembly of the Hanoi tower, passing through different points linearly interpolated with each other, taking into account the possible obstacles that the manipulator may encounter to avoid collisions. In the implementation performed, it was evidenced that the robot movement was more stable when a larger number of points were used for linear interpolation, due to the fact that the speed of the servomotors cannot be directly controlled. For this reason, if the distance between the points implied an angular displacement greater than 15°, the structure presented mechanical stability problems.

By integrating the pneumatic circuits, the image processing and the manipulator robot, the assembly process of the Hanoi tower can be carried out semi-automatically, taking into account the necessary requirements to complete the task. When transporting parts by means of pneumatic actuators, it is necessary to consider a higher pressure than necessary, given that if at some point there is a drop in pressure the system does not considerably affect the process being carried out.

References

[1] IFR, “Definition of Industrial Robot.” [Online]. Available: https://ifr.org/industrial-robots

[2] A. A. Malik and A. Bilberg, “Collaborative robots in assembly: A practical approach for tasks distribution,” Procedia CIRP, vol. 81, pp. 665–670, 2019.

[3] P. Andhare and S. Rawat, “Pick and place industrial robot controller with computer vision”, Proc. - 2nd Int. Conf. Comput. Commun. Control Autom. ICCUBEA 2016, Feb. 2017.

[4] J. Iqbal, Z. H. Khan, and A. Khalid, “Prospects of robotics in food industry,” Food Sci. Technol., vol. 37, no. 2, pp. 159–165, 2017.

[5] K. H. Tantawi, A. Sokolov, and O. Tantawi, “Advances in Industrial Robotics: From Industry 3.0 Automation to Industry 4.0 Collaboration,” TIMES-iCON 2019 - 2019 4th Technol. Innov. Manag. Eng. Sci. Int. Conf., 2019.

[6] J. J. Vaca González, C. A. Peña Caro, and H. Vacca González, “Cinemática inversa de robot serial utilizando algoritmo genético basado en MCDS,” Rev. Tecnura, vol. 19, no. 44, p. 33, 2015.

[7] O. A. Vivas Alban, M. F. Piamba Mamián, and Y. E. Otaya Bravo, “Diseño y construcción de una interfaz háptica de seis grados de libertad,” Tecnura, vol. 21, no. 54, pp. 33–40, 2017.

[8] C. Ma, Y. Zhang, J. Cheng, B. Wang, and Q. Zhao, “Inverse kinematics solution for 6R serial manipulator based on RBF neural network,” Int. Conf. Adv. Mechatron. Syst. ICAMechS, vol. 0, pp. 350–355, 2016.

[9] V. Noppeney, T. Boaventura, and A. Siqueira, “Task-space impedance control of a parallel Delta robot using dual quaternions and a neural network,” J. Brazilian Soc. Mech. Sci. Eng. 2021 439, vol. 43, no. 9, pp. 1–11, 2021.

[10] M. Meghana et al., “Hand gesture recognition and voice-controlled robot,” Mater. Today Proc., vol. 33, pp. 4121–4123, 2020.

[11] P. M. Reddy, S. P. Kalyan Reddy, G. R. Sai Karthik, and B. K. Priya, “Intuitive Voice Controlled Robot for Obstacle, Smoke and Fire Detection for Physically Challenged People,” Proc. 4th Int. Conf. Trends Electron. Informatics, ICOEI 2020, pp. 763–767, 2020.

[12] G. Y. Luo, M. Y. Cheng, and C. L. Chiang, “Vision-based 3-D object pick-And-place tasks of industrial manipulator,” 2017 Int. Autom. Control Conf. CACS 2017, vol. 2017, pp. 1–7, 2018.

[13] M. Zhao, Y. Peng, L. Li, and X. Qiao, “Detection and classification manipulator system for apple based on machine vision and optical technology,” ASABE 2020 Annu. Int. Meet., pp. 1-, 2020.